16èmes Journées de l'Hydrodynamique

27-29 novembre 2018 - Marseille

FAR-FIELD MAXIMAL POWER ABSORPTION OF A BULGING CYLINDRICAL WAVE ENERGY CONVERTER: PRELIMINARY NUMERICAL RESULTS

ABSORPTION MAXIMALE EN CHAMP LOINTAIN D'UN SYSTÈME HOULOMOTEUR CYLINDRIQUE EN RENFLEMENT: RÉSULTATS NUMÉRIQUES PRÉLIMINAIRES

M. ANCELLIN[(1)], A. BABARIT[(2)], P. JEAN[(3)], F. DIAS[(1)]

Corresponding author: matthieu.ancellin@ucd.ie

[(1)]School of Mathematics and Statistics, University College Dublin, MaREI Centre, Ireland
[(2)]LHEEA, École Centrale de Nantes – CNRS, Nantes, France
[(3)]SBM Offshore, Monaco

Summary

The maximal power absorbed by a wave energy converter can be estimated from the far-field behavior of the waves radiated by the device. For realistic estimates, constraints must be used to enforce restrictions on the set of admissible motions when deriving the maximal absorption width. This work is dedicated to the numerical computation of the maximal absorption width under constraints for devices with several non-trivial degrees of freedom. In particular, the method is applied to a model of a bulging horizontal wave energy converter similar to the SBM Offshore S3 device.

Résumé

La puissance maximale absorbable par un système houlomoteur peut être estimée à partir des vagues radiées en champ lointain par le système. Pour une estimation réaliste, des contraintes doivent être appliquées sur l'ensemble des mouvements admissibles lors du calcul de la largeur de capture maximale. Ce travail est dédié au calcul numérique de la largeur de capture maximale sous contraintes pour des systèmes avec des degrés de liberté non-triviaux. En particulier, la méthode est appliquée à un modèle de système houlomoteur cylindrique se déformant en renflement, similaire au S3 de SBM Offshore.

I – Introduction

During the design phase of a wave energy converter (WEC), several analytical and numerical methods are available to estimate the power absorbable by the device. The one discussed in this paper relates the far-field waves radiated by the device to the maximal absorption width. Since it only requires the resolution of a few linear potential flow radiation problems, it is one the of simplest methods available. It has been presented and applied in [3, 8, 7, 11] among others.

By absorbable power, it is meant transmissible from the waves to a motion or deformation of the WEC, disregarding the subsequent conversion of the energy. The problem is only a fluid-structure interaction problem and the power take-off will not be discussed in this paper.

In general for a body of nontrivial shape, the far field behavior must be computed numerically with a Boundary Element Method (BEM) solver. Afterwards, the computation of the maximum capture width requires to solve an optimization problem under constraints which can be difficult to handle analytically in dimensions higher than one. The goal of this work is the development and validation of a numerical tool to help the computation of this value for any device with several degrees of freedom (dofs), including non-trivial deformation degrees of freedom. To our knowledge, no previous work considered such a general framework.

In the next section, the theoretical expression for the capture width is presented. In the following section, some aspects of the implementation of the numerical computation are briefly discussed. Then, the results of the optimization under constraint are discussed for a simple buoy with two translational degrees of freedom. Finally, in the last section of this paper, the method is applied to a model of a bulging horizontal cylinder similar to the SBM Offshore S3 device [5].

II – Expression of the maximal absorption width

Let us consider a linear potential flow in the frequency domain. For the sake of simplicity, all computations in this paper will be done assuming an infinite water depth. This paper follows the conventions of [3] [a] and we refer to it for more details on the derivation of the following formulas. In the far field, the radiated wave can be described by the complex-valued Kochin function $H(\theta)$, where θ is a direction of interest. It can be related to the complex-valued velocity potential Φ in cylindrical coordinates as

$$\Phi(R,\theta,z) = 4\pi\sqrt{\frac{1}{\lambda R}}H(\theta)f_0(z)e^{i\left(2\pi\frac{R}{\lambda}+\frac{\pi}{4}\right)} + O\left(\frac{1}{R^{\frac{3}{2}}}\right) \tag{1}$$

where f_0 is a function of the vertical coordinate z only and λ is the wavelength of the waves.

Since we consider a linear problem, the potential and the Kochin function can be decomposed as a sum of contributions from each of the degrees of freedom taken independently.

a. In particular, Newman in [11] uses a different convention for the definition of the Kochin functions : $H_{\text{Newman}} = 4\pi k\, H$, where k is the wave number. The convention for time dependence is also different : $x(t) = \Re\left(\hat{x}_{\text{Newman}}e^{i\omega t}\right)$ whereas it is $x(t) = \Re\left(\hat{x}e^{-i\omega t}\right)$ in this paper.

In frequency-domain, a motion of the body will be defined by n_{dof} complex values $\hat{a}_j$ representing the amplitude of the degree of freedom j. The phase of the complex value $\hat{a}_j$ is defined relative to the phase of the incoming wave. We can then write $H = \sum_j^{n_{\text{dof}}} \hat{a}_j H_j$ where H_j is the Kochin function for a unit excitation of the dof j.

By writing an energy balance around a WEC [3, Eq. 4.21], we can derive an expression for the absorption width. Assuming a WEC oscillating in waves with complex-valued dof amplitudes $\hat{a} = (\hat{a}_1, \dots, \hat{a}_{n_{\text{dof}}}) \in \mathbb{C}^{n_{\text{dof}}}$, the absorption width reads :

$$W(\hat{a}, k, \beta) = 8\pi k \Im\left(\sum_{j=1}^{n_{\text{dof}}} \hat{a}_j H_j^*(k, \pi + \beta)\right) - 8\pi k^3 \int_0^{2\pi} \left|\sum_{j=1}^{n_{\text{dof}}} \hat{a}_j H_j(k, \theta)\right|^2 d\theta \,, \tag{2}$$

where $\Im$ is the imaginary part, the star denotes the complex conjugate, k is the wave number and β is the direction of the incoming waves (in radian).

Since the phase of $\hat{a}_j$ is given relative to the phase of the incoming waves, the first term of (2) depends on the difference of phase between the WEC motion and the incoming waves. The second term of (2) is the total amount of energy lost by radiation by the WEC in all directions and is independent of this difference of phase.

For a given motion of the WEC, this first term varies with the difference of phase as a sine function between $-8\pi k \left|\sum_j \hat{a}_j H_j^*\right|$ and $8\pi k \left|\sum_j \hat{a}_j H_j^*\right|$. When we are looking for the best capture width, the difference of phase can be assumed to be optimal and the first term maximal. We will denote this situation as the WEC being *in phase* with the incoming waves.

The diffraction does not appear explicitly in (2). Physically, it can be understood by the fact that no energy can be absorbed by a fixed non-radiating body. Mathematically, we refer to [3, Eq. (4.20)].

The above expression relates a given motion of the WEC to the power absorbable by this motion. The maximum absorbable power can be found as the maximum over all possible motions of the body. The optimal capture width reads :

$$W^{\text{optimal}}(k, \beta) = \max_{\hat{a} \in \mathbb{C}^{n_{\text{dof}}}} \left[W(\hat{a}, k, \beta)\right] = \max_{\hat{a} \in \mathbb{R} \times \mathbb{C}^{n_{\text{dof}}-1}} \left[W^{\text{in phase}}(\hat{a}, k, \beta)\right] , \tag{3}$$

where $W^{\text{in phase}}$ is defined as

$$W^{\text{in phase}}(\hat{a}, k, \beta) = 8\pi k \left|\sum_{j=1}^{n_{\text{dof}}} \hat{a}_j H_j^*(k, \pi + \beta)\right| - 8\pi k^3 \int_0^{2\pi} \left|\sum_{j=1}^{n_{\text{dof}}} \hat{a}_j H_j(k, \theta)\right|^2 d\theta \,. \tag{4}$$

The analytical optimization of the difference of phase between the WEC and the incoming waves reduces the dimension of the space of candidate motions by one. Indeed, since this expression is independent on the global phase of $(\hat{a}_j)_j$, one of the amplitude can be taken as real in the optimization, that is $(\hat{a}_j)_j \in \mathbb{R} \times \mathbb{C}^{n_{\text{dof}}-1}$.

For a single dof ($n_{\text{dof}} = 1$), the absorption width W is a quadratic function of $|\hat{a}|$, where $\hat{a}$ is the complex-valued amplitude of the dof. This function has a maximum $|\hat{a}|^{\text{optimal}}$ that reads (see also [11]) :

$$|\hat{a}|^{\text{optimal}}(k, \beta) = \frac{1}{2k^2} \frac{|H(k, \pi + \beta)|}{\int_0^{2\pi} |H(k, \theta)|^2 d\theta}, \qquad W^{\text{optimal}}(k, \beta) = \frac{2\pi}{k} \frac{|H(k, \pi + \beta)|^2}{\int_0^{2\pi} |H(k, \theta)|^2 d\theta} \tag{5}$$

Using the assumption of a slender body, Newman [11] and Farley [7] have derived analytical expressions for the maximal capture width for a deformation along a single degree of freedom.

A generalization of (5) for several degrees of freedom can be found in [3, Eq. 4.24]. It takes the form of a complex-valued linear system of n_{dof} equations, since the function to maximize has the form of a quadratic function of $\hat{a}$.

In the rest of this paper, we will also use the following relation derived by [6] :

$$\frac{k}{2\pi}\int_{-\pi}^{\pi} W^{\text{optimal}}(k,\beta)\,d\beta = n_{\text{dof}}, \tag{6}$$

where n_{dof} is the number of hydrodynamically independent degrees of freedom (that will not be distinguished from the total number of degrees of freedom in this paper).

However, the amplitude at which this absorbed power is maximal is often not reachable by the devices. The amplitude is constrained by, for instance, mooring for translation motion or elastic properties of the material for a deformable WEC. The range on which the electric system can extract energy can also constrain the "useful" amplitude of the dof. In this paper, we are interested in this more realistic case where the maximal amplitude is constrained.

For a single degree of freedom, the constraint can easily be taken into account in the analytical expression (5) (see also [11]) :

$$|\hat{a}|^{\text{optimal}}(k,\beta) = \min\left(\frac{1}{2k^2}\frac{|H(\pi+\beta)|}{\int_0^{2\pi}|H(\theta)|^2 d\theta}, |\hat{a}|^{\text{constr}}\right), \quad W^{\text{optimal}}(k,\beta) = W(|\hat{a}|^{\text{optimal}},k,\beta) \tag{7}$$

where $|\hat{a}|^{\text{constr}}$ is the maximal admissible amplitude.

For several degrees of freedom, an optimization under constraint problem has to be solved. Using (4), the optimization problem will happen in $\mathbb{R}\times\mathbb{C}^{n_{\text{dof}}-1} \equiv \mathbb{R}^{2n_{\text{dof}}-1}$.

It might be possible to derive an analytical expression for the optimal capture width under constrain as in the 1D case, at least for simple constraints. This has not be done in this work, where we used an optimization algorithm to find the optimum.

III – Implementation

In [11], an analytical model had been used to compute the radiated wave field of an elongated body, by making the approximation of a slender body. We have chosen here instead to base our work on full 3D linear potential flow simulations using the open source boundary element method solver Nemoh [4]. This will allow to directly use this method on a larger variety of body shapes.

However, solving a 3D BEM problem might be relatively slow, particularly in comparison with an analytical model. According to the benchmark of [12], Nemoh is also noticeably slower than its commercial concurrent WAMIT. In parallel of this work, an effort is being made to speed up the computations with Nemoh in a refactored version under development [1, 2] at UCD.

After the Kochin functions have been computed by solving a linear potential flow problem, the maximum capture width must be found by solving an optimization problem under constraint. They were solved using the off-the-shelf optimization tools from Scipy [9]. It relies on the SLSQP (Sequential Least Squares Programming) algorithm as implemented by [10].

The optimizations for several wave frequencies or several incoming wave directions are "embarrassingly parallel" problems and can straightforwardly be run in parallel.

Since we want to maximize a quadratic function within a convex domain, no convergence difficulty is expected for the optimization algorithm, as long as the constraint is smooth enough. On cases with a low number of degrees of freedom, the solution of the optimization algorithm has been validated by comparing with a brute force research of the optimum.

The computations were run on a high-end desktop from 2012 (Intel i7-3770K CPU) using 4 threads in parallel. Depending on the refinement of the mesh and the number of degrees of freedom, the computations of the following results took from a minute to an hour.

In the course of the preparation of this paper, an attempt was made to reproduce the slender bodies analytical results from [11] using the numerical code. Difficulties were encountered. Convergence problem with Nemoh have been noticed before (in [5]) for a cylinder close to the free surface. Some more work is necessary to check whether the discrepancies that we noticed are due to this known problem, to the hypothesis of a slender body or to another problem in the implementation.

IV – Illustration on a simple test case

In the next paragraph, we will study the case of a simple buoy. We consider a vertical cylinder of diameter 1 m and wet height 1 m. This body will be allowed to move in translation only, with two degrees of freedom (heave and surge). The rotation degrees of freedom have be neglected for the sake of simplicity.

At first, the body is allowed to move in one degree of freedom at a time. If $\hat{x}$ is the complex-valued amplitude associated with the coordinate of the body $x(t)$, then

$$|\hat{x}| = \max_t |x(t)|.$$

For a single degree of freedom, the constraint on the maximal displacement of the body can straightforwardly be expressed as a constraint on $\hat{x}$:

$$|\hat{x}| \leq A \tag{8}$$

for some maximal amplitude A.

The dimensionless absorption width has been plotted on Figure 1 for several maximal amplitudes of motion. For an axisymmetric problem, the relation (6) implies $k\,W = n_{\mathrm{dof}}$. Since the buoy moving in heave is an axisymmetric problem, the dimensionless absorption width without constraint is 1 for all incoming wave directions and all wavelengths. For surge, the dimensionless absorption width is 2 (independently of the wavelength) for waves traveling in the x-direction ($\beta = 0$, $\beta = \pi$), 0 for waves traveling in the y-direction ($\beta = \frac{\pi}{2}$, $\beta = \frac{3\pi}{2}$) and 1 on average over all wave directions (see also Figure 3).

When the motion of the body is constrained, the absorption width is lower. For high wavelengths, reaching the absorption width of the unconstrained case would require large motions of the body.

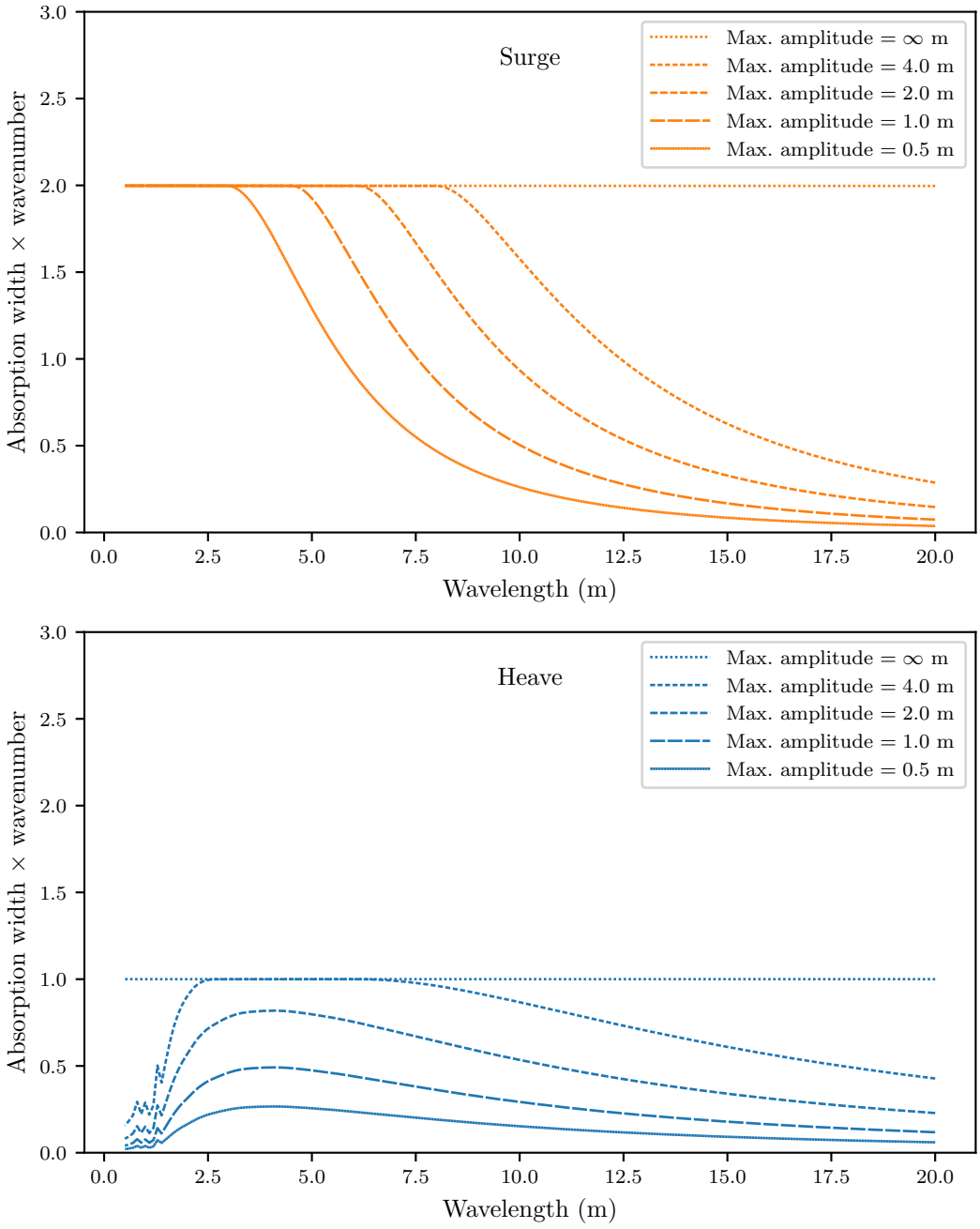

FIGURE 1 – Dimensionless maximal absorption width of a floating vertical cylinder as a function of the wavelength of the incoming waves for several constraints on the motion of the body (maximal amplitudes A as in (8)). The incoming waves are traveling in the direction of the x-axis. The body moves along a single degree of freedom (on top : surge, on the bottom : heave).

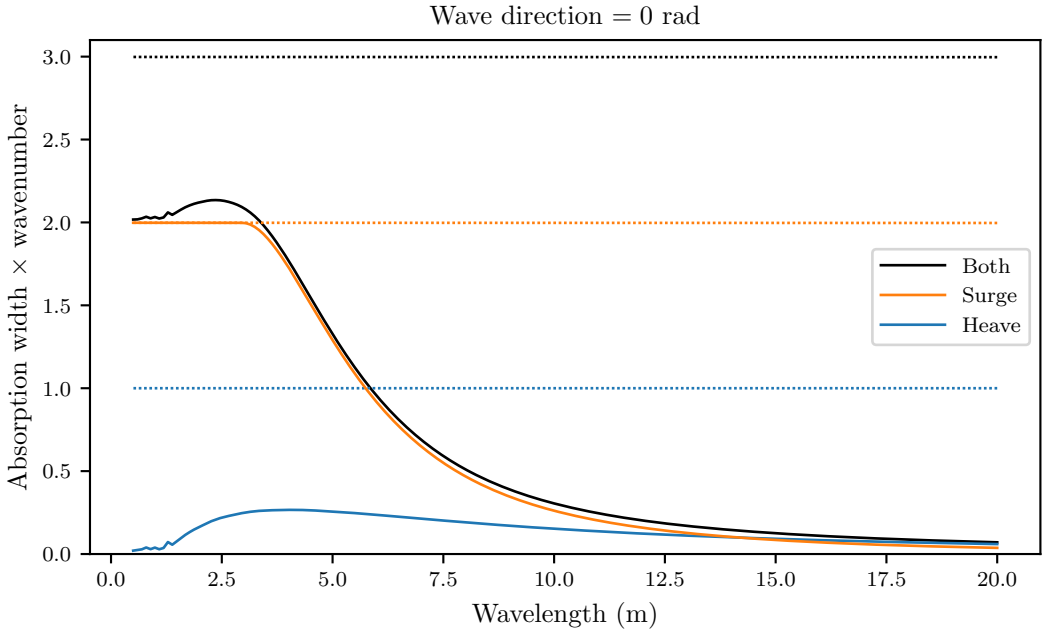

FIGURE 2 – Dimensionless maximal absorption width of a floating vertical cylinder as a function of the wavelength of the incoming waves for several degrees of freedom and for two different constraints on the motion of the body (in plain line : constraint (10) with $A = 0.5\,\mathrm{m}$, in dotted line : unlimited motion). The incoming waves are traveling in the direction of the x-axis.

The natural extension of the constraint (8) to several degrees of freedom is to limit the displacement of the dof as

$$\max_t d(t) \leq A\,, \tag{9}$$

where $d(t) = \sqrt{x(t)^2 + z(t)^2}$ is the displacement of the body with respect to its rest position. However, it is not straightforward to express the displacement $d(t)$ as a function of $\hat{x}$ and $\hat{z}$. Thus, for the sake of simplicity, the constraint on the motion with two degrees of freedom has been chosen instead as

$$\sqrt{(\max_t x(t))^2 + (\max_t z(t))^2} = \sqrt{|\hat{x}|^2 + |\hat{z}|^2} \leq A. \tag{10}$$

Since

$$\max\left(\max_t x(t)^2, \max_t z(t)^2\right) \leq \max_t d(t)^2 \leq (\max_t x(t))^2 + (\max_t z(t))^2$$

the constraint (10) is more restrictive that (9), in the sense that (9) is fulfilled whenever (10) is.

In Figure 2 and Figure 3, the absorption width of the motion under two degrees of freedom has been considered. The results are plotted for two constraints :

- in dotted line, the motion is without any constraint. The absorption widths of the two individual degrees of freedom can be linearly summed to get the absorption width of the case with two degrees of freedom.
- in plain line, the constraint is given by (10) with $A = 0.5\,\mathrm{m}$. This constraint introduced a non-linearity in the model. The absorption width of the individual degrees of freedom cannot be summed anymore. The total absorption width is just slightly higher than the maximum of the individual absorption width.

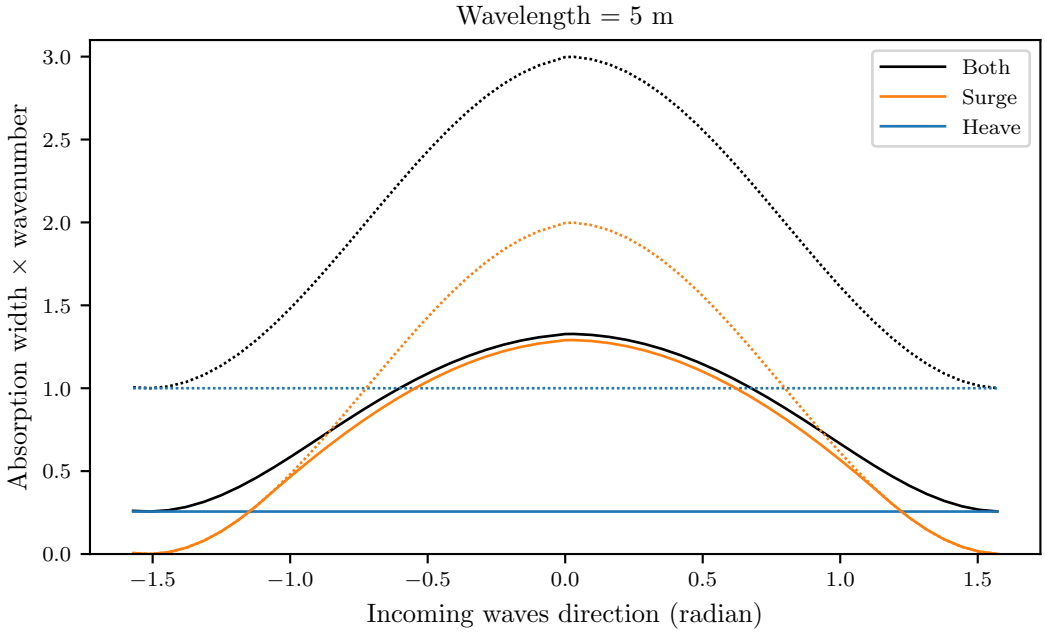

FIGURE 3 – Dimensionless maximal absorption width of a floating vertical cylinder as a function of the direction of the incoming waves for several degrees of freedom and for two different constraints on the motion of the body (in plain line : constraint (10) with $A = 0.5\,\mathrm{m}$, in dotted line : unlimited motion). The wavelength of the incoming waves is $5\,\mathrm{m}$.

Other constraints have been tested, such as

$$\max\left(\max_t x(t), \max_t z(t)\right) = \max\left(|\hat{x}|, |\hat{z}|\right) \leq A, \tag{11}$$

which is less restrictive than (9). Results are qualitatively similar, although the numerical output is much noisier. The reason is thought to be that the optimization algorithm assumes a smooth constraint and the supremum norm of (11) is not as smooth as the 2-norm of (10).

V – Application to a bulging cylinder

Finally, the code will be applied to a model of a bulging cylindrical wave energy converter. It is meant to be a rough model of the S3, described in more details in [5]. This device is an immersed horizontal cylinder made of an elastic material and filled with water. In waves, the elastic membrane is deformed and an electroactive polymer can produce electricity.

In [5], the deformation modes of the cylinder are derived. In the present work, we will consider simpler bulge deformation modes, for the sake of simplicity. The radius of the cylinder r at abscissa x and time t is given by

$$\delta r(x,t) = r(x,t) - r_0 = \Re\left(\sum_{j=1}^{n_{\mathrm{dof}}} \widehat{\delta r}_j \sin\left(j\frac{2\pi x}{L}\right) e^{-i\omega t}\right) \tag{12}$$

where r_0 is the radius at rest, $\widehat{\delta r}_j$ is the complex amplitude of the mode j and L is the length of the cylinder.

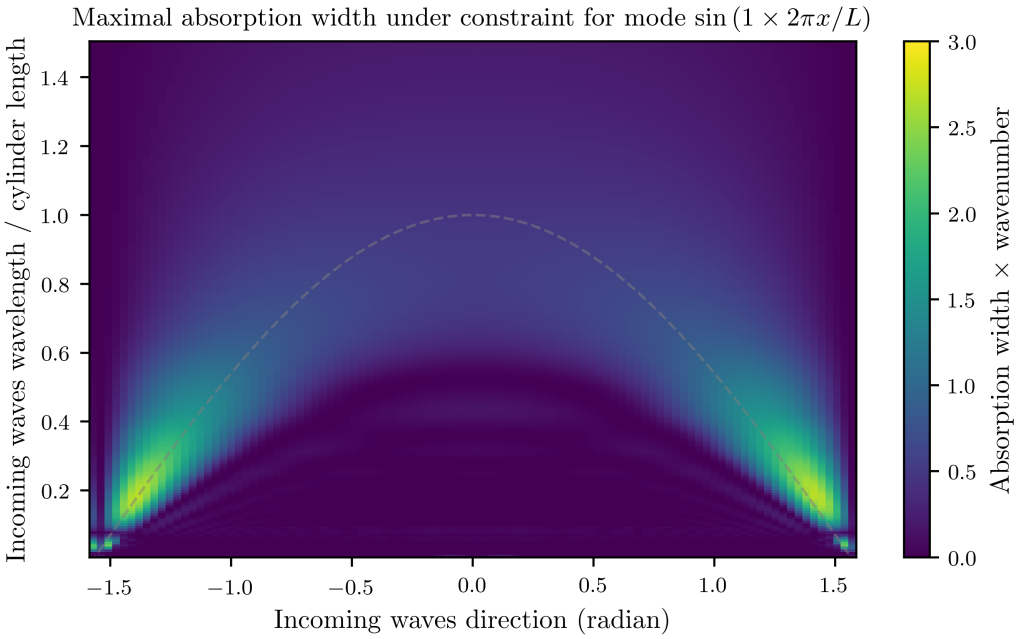

FIGURE 4 – Dimensionless maximal absorption widths as a function of the wavelength and the direction in the incoming waves for the bulging mode $\sin(2\pi\, x/L)$ with constraint (13). The dashed gray line is the curve $\cos(\beta)$ where β is the incoming wave direction.

In the following computations, a cylinder of radius 0.2 m and length 10 m (those are the dimensions of the small scale experimental model of [5]) is immersed such that its center is at $z = -0.3$ m.

The computation under constraints requires an estimate of the maximal deformation physically sustainable by the WEC. For the S3, this estimate requires the study of the elastic properties of the material and is out of the scope of this work. For this paper, an arbitrary constraint will be taken. The optimization algorithm currently in use has been noticed to give more reliable results with a smooth constraint. Then, the following constraint has arbitrarily been chosen :

$$\sum_j \left|\widehat{\delta r}_j\right|^2 \leq \left(\frac{r_0}{2}\right)^2 . \tag{13}$$

Other constraints than (13) have been tested, in particular to try to limit directly the maximum radius or its derivative. However, as for the floating buoy of Section IV, results appear to be noisier when a supremum norm is used, probably due to the algorithm for the optimization under constraints. More work is necessary to have a code able of handling arbitrary constraints.

In Figure 4, a map of the absorption width under constraint for a single mode of deformation has been plotted. When the incoming waves travel in the same direction as the cylinder ($\beta = 0$), the best absorption width is reached for wavelengths closeeto the wavelength of the deformation mode of the WEC (here that is $\lambda = L$). When the incoming waves arrive sideways at the WEC, the wavelength at which the capture is maximal gets lower. It corresponds to the wavelength of the body deformation mode as seen by the transverse incoming waves $\cos(\beta)L$ where β is the incoming wave angle.

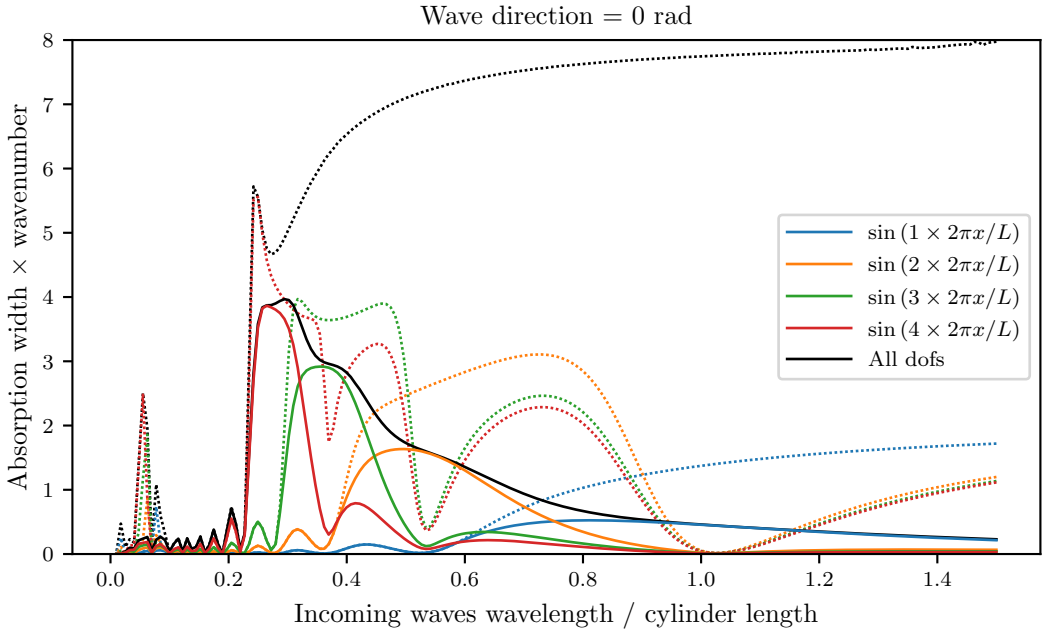

FIGURE 5 – Dimensionless absorption width as a function of the wavelength of the incoming waves. The colored lines correspond to the absorption width of the different degrees of freedom taken individually, while the black line corresponds to the absorption width of a cylinder with all four degrees of freedom. Dotted lines corresponds to cases without constraint on the deformation. Plain lines corresponds to cases with constraint (13).

At shorter wavelengths, there are less angles at which the absorption width is non-zero. However, when it is non-zero, its value is much higher than the typical value at higher wavelength. This can be seen as an indirect consequence of (6).

In Figure 5 and 6, the absorption width with and without constraint has been plotted for four sinusoidal modes of deformation and for the combination of all four.

In Figure 5, the absorption width of a mode is centered around the wavelength of the wave corresponding to the wavelength of the deformation mode. This is true in particular for constrained absorption widths. Unconstrained modes can present high absorption width at other wavelengths (for instance the mode $\sin(4 \times 2\pi x/L)$ near $\lambda = 0.8$ – see dotted red curve), but their disappearance in the constrained case (plain red line) seems to indicate that they do not correspond to a realistic deformation.

Some high peaks can be seen for the unconstrained modes for low wavelengths. They disappear in the constrained case and must thus be unrealistic deformations.

Finally, the black curve of the absorption width for the four dofs combined shows a much lower value when the deformations are constrained, since the deformations of the individual modes cannot pile up anymore. With the constraint (13), the total absorption width seems close to the convex hull of the individual constrained absorption widths.

Since the total deformation is limited, adding more modes could have had no effect on the total absorption width. Instead, since the deformation modes are effective for different wavelengths of the incoming waves, they do not compete with each other. Then, adding more modes just increases the range of wavelengths for which the cylinder can capture energy.

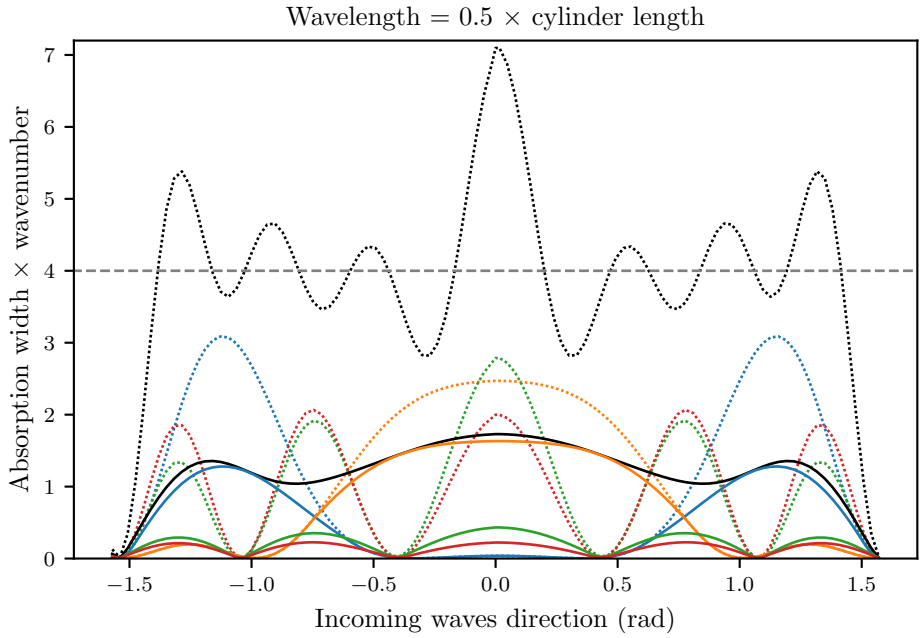

FIGURE 6 – Dimensionless absorption width as a function of the direction of the incoming waves (in radian) for waves with wavelength $L/2$. The legend is the same legend as for Figure 5 : the colored lines correspond to the absorption width of the different degrees of freedom taken individually, while the black line corresponds to the absorption width of a cylinder with all four degrees of freedom. Dotted lines correspond to cases without constraint on the deformation. Plain lines correspond to cases with constraint (13). The horizontal dashed gray line corresponds to the theoretical average value based on (6).

The maximal absorption width becomes higher for modes with lower wavelength of deformations. This effect is partially due to the choice of the constraint (13) since it limits only the radius of the cylinder. A more realistic constraint would also limit the derivative of the radius with respect to x, thus reducing the absorption width of the modes with low wavelengths.

In Figures 6, the absorption width has been plotted as a function of the direction of the incoming waves, for the same degrees of freedom, for the wavelength corresponding to half of the cylinder length. At this wavelength, the mode $\sin(2 \times 2\pi x/L)$ in orange is the most active, with the mode $\sin(1 \times 2\pi x/L)$ in blue for wave coming sideways. Other modes may contribute in the unconstrained case, but their contribution might require an unrealistically large deformation, since they almost disappear when a constraint is applied.

In the unconstrained case, the total absorption width in dotted black line can be compared with the theoretical average value based on (6) in dashed gray line.

VI – Conclusion

In this paper, a first exploration of the computation of the maximal absorption width from the far-field radiation behavior of a WEC has been presented. The end goal of this study is the development of generic numerical tools for the design of WECs, including devices with non-trivial degrees of freedom.

For a realistic modeling with this method, an upper bound for the body motion or deformation has to be introduced in the computations. The constraints used in this paper may not be totally meaningful from a physical point of view. The optimization under constraint problem should be studied more closely to get a better understanding of the best way to apply a realistic constraint. More realistic constraints could include not only limitations of the amplitude of the motion, but also of its velocity.

This approach has been illustrated in this paper by an application to a rough model of the SBM bulging cylindrical wave energy converter. More deformations modes should be introduced in the model in the future (including for instance cosine modes of deformation or the actual modes of the S3 as derived in [5]). Then parametric studies could be done with this model to understand the role of the radius of the cylinder or of the depth at which it is immersed.

Acknowledgments

This work is funded by Science Foundation Ireland (SFI) under Marine Renewable Energy Ireland (MaREI), the SFI Centre for Marine Renewable Energy Research (grant 12/RC/2302). The authors also acknowledge the support of SBM Offshore.

Références

[1] M. Ancellin and F. Dias. Using the floating body symmetries to speed up the numerical computation of hydrodynamics coefficients with Nemoh. In *Proceedings of the 37th International Conference on Ocean, Offshore and Arctic Engineering (OMAE2018)*, Madrid, Spain, 2018.

[2] M. Ancellin et al. Capytaine : a Python-based rewrite of Nemoh. `DOI:10.5281/zenodo.1426306`.

[3] A. Babarit. *L'énergie des vagues : Ressource, technologies et performance*. ISTE éditions, 2018.

[4] A. Babarit and G. Delhommeau. Theoretical and numerical aspects of the open source BEM solver NEMOH. In *Proceedings of the 11th European Wave and Tidal Energy Conference (EWTEC2015)*, Nantes, France, 2015.

[5] A. Babarit, J. Singh, C. Mélis, A. Wattez, and P. Jean. A numerical model for analysing the hydroelastic response of a flexible electro active wave energy converter. *Journal of Fluid and Structures*, 74 :356–384, 2017.

[6] J. Falnes and A. Kurniawan. Fundamental formulae for wave-energy conversion. *Royal Society open science*, 2(3) :140305, 2015.

[7] F. Farley. Wave energy conversion by flexible resonant rafts. *Applied Ocean Research*, 4(1) :57–63, 1982.

[8] F. Farley. Far-field theory of wave power capture by oscillating systems. *Philosophical Transactions of the Royal Society A : Mathematical, Physical and Engineering Sciences*, 370 :278–287, 2012.

[9] E. Jones, T. Oliphant, P. Peterson, et al. SciPy : Open source scientific tools for Python, 2001–. `http://www.scipy.org/` [Online ; accessed 3rd October 2018].

[10] D. Kraft. A software package for sequential quadratic programming. *Forschungsbericht- Deutsche Forschungs- und Versuchsanstalt fur Luft- und Raumfahrt*, 1988.

[11] J. Newman. Absorption of wave energy by elongated bodies. *Applied Ocean Research*, 1(4) :189–196, 1979.

[12] M. Penalba Retes, T. Kelly, and J. Ringwood. Using NEMOH for modelling wave energy converters : A comparative study with WAMIT. In *Proceedings of the 12th European Wave and Tidal Energy Conference (EWTEC2017)*, Cork, Ireland, 2017.